Nanostructuration of Polyamide 6/Polyetheramines Blends by Reactive Extrusion: Reducing Viscosity While Improving the Tensile Properties

Mathilde Auclerc, Amélie Bru-Chambet, René Fulchiron, Guillaume Sudre, Nicolas Garois, Philippe Cassagnau, Véronique Bounor-Legaré

Nano-structuration of polyamide6/polyetheramines blends by reactive extrusion: Reducing viscosity while improving the tensile properties

Mathilde Auclerc[a], Amélie Bru-Chambet[a], René Fulchiron[a], Guillaume Sudre[a], Nicolas Garois[b], Philippe Cassagnau[a], Véronique Bounor-Legaré[a]*

[a] Université Claude Bernard Lyon 1, CNRS, INSA Lyon, Université Jean Monnet, UMR 5223,Ingénierie des Matériaux Polymères, F-69622 Villeurbanne Cedex, France

[b] Hutchinson, Centre de Recherche, Rue Gustave Nourry - B.P. 31, 45120 - Chalette-sur-Loing, France

Corresponding author* : bounor@univ-lyon1.fr

Abstract

Nanostructurated polyamide-based blends were synthetized by reactive extrusion with multifunctional amine-terminated polyethers in a twin-screw extruder. All the reactive blend exhibited a noticeable reduction of the viscosity (up to 50 %) while only the systems synthetized with a small amount of the trifunctionnal Jeffamine® T-403 (0.7 wt%) depicted an increase of the Young's modulus and yield strength by 20 % and 13 %, respectively, compared to the neat polyamide. The amorphous phase mobility and tensile properties modifications were explained by the crystalline nano-structure evolution of the chemically modified polyamide-6 (PA6). For the smallest quantity of amine, chains mobility evolutions in the amorphous phase of the blends PA6/T-403 were associated to the MAF (mobile amorphous fraction)/RAF (rigid amorphous fraction) ratio. The material stiffening was related to due to a higher RAF content but also to thicker crystalline lamellae. On the contrary, a difunctional diamides, Jeffamine® D-400, led to chains scissions with no modification of the RAF content.

I) Introduction

Thermoplastic polyamides are used in a large variety of industrial applications thanks a good price/performance ratio with a good compromise between the mechanical and thermal properties. In addition, polyamides have good wear resistance due to a low coefficient of friction and excellent resistance to various solvents, oils and bases [1-3]. However, in accordance with the targeted application and the process used, some properties have to be improved. As an example, the injection-molding of complex parts with thin walls or those containing fillers are complicated to execute. Moreover, in terms of environmental protection, it is preferable to use low viscosity fluids which increase the facility of process rates and so decrease the energy consumption for processing. The decrease of the molar mass by chain scissions or through the oligomers synthesis led to a decrease of the viscosity [4]. Using this strategy, the processability of such polymer matrices was improved but, in the same time, a concomitant loss in mechanical properties was observed. Researches to overcome this limitation proposed for example the synthesis of controlled star-branched architecture polymers [5-9] or the incorporation of small quantities of such structures into virgin matrix as additives [10-16]. Both solutions led to unusual properties compared to linear and unmodified polymer with the same M_n. Indeed, the viscosity decreased (if the branch molar mass is below the entanglement molar mass) while the solid-state mechanical properties of the material were hardly affected. As an example, Fu and coworkers [8] synthetized a star-shaped polyamide-6 (PA6) in an autoclave using three concentrations of trimesinic acid to vary the branched-chains length. The viscosity in melt and in solution of star-shaped PA6 decreased in comparison with the one of the linear polymer with almost similar molar mass. These results were explained by the smaller molecular dimension and the lower ability to create hydrogen bonding for branched polymer. For branches with a number-average molar mass around 9,600 $g.mol^{-1}$, the relative viscosity decreased from 2.6 to 2.0 while the Young's modulus, the Izod impact strength and the tensile strength were maintained except for the elongation at break which decreased from 260 to 160 %. Run et al. [10] studied the introduction of small amount of hyperbranched poly(amide-ester) in poly(butylene succinate) (HBP/PBS) and its impact on the physico-chemical properties. They demonstrated the reinforcement character of the HBP through the characterization of the mechanical and rheological properties. Fewer entanglements in the blends led to important complex viscosity drop, while the Young's modulus and the impact strength were improved thanks to numerous hydrogen bonds between the hydroxyl groups of the additive and the ester groups of the matrix. The best results were obtained for 2 wt% of HBP. In this particular case, the complex viscosity decreased by 12 % while the Young's modulus and the tensile strength increased by 8.5 and 1.2 MPa respectively. These solutions clearly improved the balance between the material processability and its mechanical performances.

However, the synthesis of well-designed/regular branched polymeric chain architectures are hardly manufactured at industrial scale. As an alternative, randomly branched structures can

be obtained by adding a multi-functional reactive agent to a compatible polymer. Only few papers dealt with the synthesis of these kinds of structures and their influences on the physico-chemical properties. Steeman and his team [17] synthetized, in autoclave, linear and branched polyamides varying the number of branching points per chain (from 0.21 to 0.48 branching points/chain) and the length of the branches. The random branched structures were synthetized by introducing multi-functional monomers [1,6-hexane diamine and tri-functional 6,6',6''-(1,3,5-triazine-2,4,6-triyltriimino)tri-hexanoic acid (TCAM)] as branching agent, to the reactional medium for the caprolactam polymerization. The synthesis conditions were drastic (270 °C and 5 bar) and required at least 5 hours. The viscosity evolution was observed to be different and was attributed to the long chain branching able to promote numerous entanglements. Thus, in this case, the branched materials displayed an equivalent viscoelastic behavior to the linear materials but with an higher molar mass compared to branched ones. In addition, the branched polyamide exhibited a stronger shear thinning behavior. An interesting result for processing was that branched polymers with the same zero shear viscosity as the linear one exhibits a lower viscosity at high shear rates (from 300 to 200 Pa.s for the linear and branched respectively at 10^3 s^{-1}). The decrease of the viscosity at high shear rate through the generation of a long-chain branched PA6 based structure was also observed by Cai et al.[18]. The rheological and mechanical behaviors of PA6 chain extended in the melt with low concentration (max 2 wt%) of specifically synthetized multi-epoxy derivatives was studied. The authors underlined both viscosity increase and decrease depending of the range of tested shear rate associated to excellent mechanical properties. As a result and according also to the work realized by Seo et al. [19], specific viscosities can be adapted by incorporating various numbers of branches of different lengths. Besides these approaches based on either the addition of a branched structures to a polymer or the synthesis of a new branched polymer, we recently developed a new method to obtain a decrease of viscosity coupled with an increase of tensile properties by a one-step reactive extrusion step [20]. An increase of the Young's modulus up to 30 % coupled with a decrease of the zero shear viscosity (from 300 Pa.s to 20 Pa.s) of a copolyether-ester COPE matrix was achieved through reactive extrusion with 2 wt% of Jeffamine® T-403. A deeper analysis of the created structure evidenced the formation of branched species responsible of the processability enhancement. In another study, Auclerc et al. [21] revealed that a PA6 modified by reactive extrusion using Jeffamine® T-403 is composed of a mixture of randomly branched and linear molecules. Furthermore, the creation of these branched structures led to the modification of the amorphous phase mobility by controlling the nanostructure morphology of the material, particularly the crystalline lamellae thickness and the rigid amorphous fraction (RAF) content.

The present work focus on the relationships between the chemical modification of the PA6 by different Jeffamine® and their thermal, crystallization and mechanical behaviors. The aim of this study is to demonstrate the crucial role of random branching on the balance between viscosity/processability and tensile properties of the modified material. For this purpose, a diamine additive with similar molar mass was studied in the same way to highlight the

importance of using an additive with functionality over 2 to impact the amorphous phase mobility. Finally, this study will be devoted to explain the existing links between the physico-tensile properties versus the nanostructure of the material.

II) Materials and Formulations

II-a) Materials

The PA6 matrix Akulon F136DH® was kindly provided by DSM as polymer pellets. The number-average molar mass was found to be 51,000 $g.mol^{-1}$ by using a size exclusion chromatography in hexafluoroisopropanol (HFIP) and with poly(methyl methacrylate) (PMMA) as a standard. Chain end-groups titration on PA6 gave a molar mass at 30,800 $g.mol^{-1}$. The melting point for PA6 was measured at 219 °C and the decomposition temperature was found to be 445 °C by using DSC and TGA respectively.

The reagent Jeffamine® T-403 from Huntsman was supplied by Hutchinson Research Center. The diamine Jeffamine® D-400 were purchased from Sigma Aldrich. Their main characteristics are given in Table 1.

Table 1: Characteristics of the three polyetheramine reagents (Jeffamine®)

Reagents	Chemical structures	n (degree of polymerization) [(a)]	M_n ($g.mol^{-1}$) [(a)]
D-400	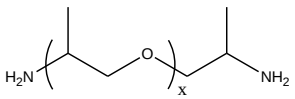 n = x	5.91	417
T-403	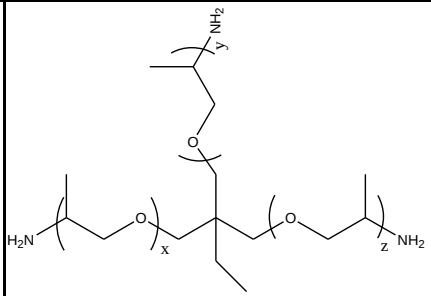 n = x+y+z	5.10	427

[(a)] *Average values obtained by ^1H NMR in $CDCl_3$ and MALDI-TOF MS analyses [21]*

II-b) Samples preparation

PA6 pellets were first dried under vacuum for 24 h at 80 °C to remove water prior to use. The reactive extrusion was performed in a co-rotating twin-screw extruder (Leistriz LSM model, L/D = 34, D = 34 mm) at 245 °C. The twin-screw profile is shown in Figure 1.

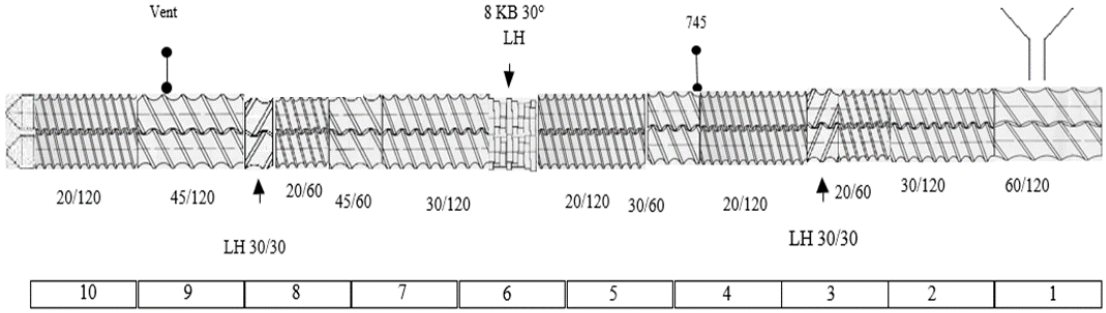

Figure 1: Twin-screw profile with two left-handed (LH) conveying elements. Each barrel element is denominated by two figures (the first number is the pitch of screw, and the second is the screw length), KB means Kneading Block with an angle between them of 30°

The triamine and diamine reagents were added into the molten matrix at the injection point 745 mm and at different flow rates using an external liquid pump in order to introduce a precise quantity of amine (Table 2). PA6 was incorporated by the hopper and processed at a flow of 3 $kg.h^{-1}$ with a screw speed of 200 rpm. At the end of the extruder, samples were air-cooled down with air and granulated. Under these processing conditions, the mean residence time of the polymer in the extruder was estimated to be of 90 s.

Table 2: Molar concentrations for the different reactive blends PA6/triamine and PA6/diamine ($mol.kg^{-1}$of blend)

Reactive blends	**Reagent concentrations (wt%)**	$[NH_2]_{added}$	$[COOH]_{polyamide}$	$[NH_2]_{added}/[COOH]_{polyamide}$
PA6/D-400	1.0	0.050	0.032	1.56
	2.9	0.140	0.032	4.38
PA6/T-403	0.70	0.050	0.032	1.56
	2.0	0.140	0.032	4.38

All the samples were injected using a hydraulic injection molding machine Babyplast 6/10P equipped with a piston diameter of 14 mm and presenting a clamping force of 62 kN. The molds (dumbbell, disks, bars…) were adapted to the characterization. Chamber temperature was set at 260 °C, mold temperature at 80 °C and the injection pressure at 70 bar. The injected specimens were dried under vacuum at 80 °C for 24 h before being characterized. Rheological characterizations were carried out on disk-shaped samples (diameter of 25 mm and thickness of 2 mm). DSC experiments were performed on samples

cut out of dumbbell specimen (shaped H2) samples. SAXS and WAXS measurements were made on similar specimen as for the DSC analyses.

III) Methods of characterization

III-a) Viscosity in solution

A Ubbelohde LAUDA viscosimeter was used to determine the viscosity of polymers in solution. The solvent was formic acid (85 wt%) at 25 °C. A stock solution of each sample was prepared at a concentration around 10 $mg.mL^{-1}$ and 5 consecutive dilutions were programed. For every concentration, the viscosimeter measures the time it takes for the liquid to pass through two calibrated marks of the tube (K = 0.01 and D = 0.63 mm). Initially, the viscosity average molar mass (M_v) was measured with an Ubbelohde type viscometer for each concentration of T-403 added into PA6. To be sure that unreacted T-403 molecules did not induce modifications of the intrinsic viscosity values measured, preliminary tests were implemented. Thus, the intrinsic viscosity of solutions prepared from PA6 and T-403 blends without reaction was measured in order to ascertain that the reagent alone does not affect the measurement.

III-b) Size Exclusion Chromatography (SEC)

Molar masses of the different formulations were measured at 35°C by the SEC Acquity advanced chromatography from Waters with a RI detector (Agilent-RI-1100). Three columns were used: Apc XT 450, 125 and 45. HFIP was the eluent with a flow rate of 0.3 $mL.min^{-1}$. Samples (around 10 mg) were first solubilized several hours in 1 mL of HFIP and filtered. Approximately 20 µL was injected into the column. The average molar masses M_n and M_w were determined using PMMA as standard.

III-c) Rheological characterization

Dynamic rheological measurements were carried out on a strain-controlled ARES rheometer (TA Instruments) under a nitrogen flow and at 240 °C. Parallel plate geometry (25 mm in diameter and 2 mm gap) was used. Dynamic shear measurements were performed by varying the frequencies from 0.03 to 100 $rad.s^{-1}$ in a controlled-strain mode under the regime of the linear viscoelasticity.

III-d) Thermal analysis: Differential Scanning Calorimetry (DSC)

Thermal properties of the formulations were characterized by DSC to study the melting and crystallization behavior using the model Q2000 (TA Instruments) equipped with a refrigerated cooling system 90. Indium was used as calibration standard. Before analysis, samples were dried under vacuum at 80 °C for 24 h. Then, 5 to 10 mg of samples cut out of dumbbell specimen (for tensile test) was weighted and put in a hermetic aluminum capsule. The value of the melting temperature (T_m), crystallization temperature (T_c) and enthalpy were measured on the first cycle applied from 20 °C to 250 °C at a heating rate of 10 °C.min^{-1}. The degree of crystallinity was calculated with the equation (1) as follows:

$$\chi_c = \frac{\Delta H_m}{\Delta H_m^o} \quad (1)$$

With, ΔH_m, the integral of the melting peak taking into account the composition and ΔH_m^o, melting enthalpy if PA6 were 100 % crystalline ($\Delta H_{mPA-6}^o = 190$ J.g^{-1}) [22].

Modulated DSC (MDSC) was implemented to measure the glass transition temperature (T_g) of the different blends, as for PA6, the heat capacity step ΔC_p (used to measure the T_g) is quite wide and weak. Approximately 15 mg of samples were introduced in a hermetic aluminum pan. Noted that, samples were dried carefully at 80 °C for 24 h under vaccum because the water absorption led to a significant decrease of the T_g and non-reproducible results. The temperature was equilibrated at - 20 °C and then increased up to 140 °C with a heating rate of 2 °C.min^{-1} with a temperature modulation of ± 4 °C every 60 s. The T_g value was determined at the midpoint of the step observed in the DSC curve and given by the TA Universal Analysis software. It was also possible to estimate the mobile amorphous fraction (MAF) using the equation (2) [23].

$$\mathrm{MAF} = \left(\frac{\Delta C_{p/exp}}{\Delta C_{p/theo}}\right) \times 100 \quad (2)$$

with, $\Delta C_{p/exp}$, the measured variation of heat capacity at the glass transition (distance between tangents at T_g) and $\Delta C_{p/theo}$, the heat capacity step for a completely amorphous polymer [$\Delta C_{p/theo}$(PA6) = 0.475 J.(g.K)$^{-1}$] [24]. The rigid amorphous fraction (RAF) can be thus deduced with the following equation (3):

$$\mathrm{RAF} = 100 - \chi_c - \mathrm{MAF} \quad (3)$$

III-e) Wide Angle X-ray Scattering (WAXS) and Small Angle X-ray Scattering (SAXS)

X-ray diffraction analysis on polymers is a non-destructive powerful technique to study crystallinity (orientation, phase, size and shape).

The measurements were carried out at the European Synchrotron Radiation Facility (ESRF) in Grenoble on the BM2-D2AM beamline. The incident photon energy was set at

16 keV and two detectors were used for SAXS (D5) and WAXS (WOS) analyses. The sample-to-detector distance was about 1.15 m for SAXS and 11.0 cm for WAXS and the beam stop had a diameter of 1 mm. The q-range calibration was made with a silver behenate (SAXS) and lanthanum hexaboride (WAXS) as standard. The two-dimensional data were corrected by considering the camera geometry, dark image reading and flat field response of the detector. Each sample was put in Kapton tape and placed at the center of the sample holder. The value obtained for the empty cell with Kapton tape was subtracted from the scattering images of the studied sample.

From the SAXS patterns, it was possible to determine the long period (L_p) from the Bragg equation (4) with the maximum peak abscissa (q_{max}) of the curve.

$$L_P = \frac{2\pi}{q_{max}} \tag{4}$$

The crystalline and amorphous lamellae thicknesses values could be calculated using the ideal lamellar two-phase structure [25] and knowing the degree of crystallinity (χ_c, obtained by DSC on dried samples) with the simplified equations (5) and (6):

$$l_c = L_p \chi_c \tag{5}$$

$$l_a = L_p(1 - \chi_c) \tag{6}$$

III-f) Mechanical characterization

Uniaxial traction measurements were carried out on dumbbell specimen (shaped H2) tensile samples using the MYS QTest/25 equipped with a 30 kN force sensor. The deformation speed was 2 $mm.min^{-1}$ to measure an accurate Young's modulus, and 50 $mm.min^{-1}$ for the measurement of the yield strength and elongation at break. At least 10 different samples were tested for each formulation in order to obtain a satisfactory standard deviation was obtained.

IV) Results and discussion

PA6 was first modified by reactive extrusion using the triamine Jeffamine® T-403 as multi-functional reactive agent. Our previous study [21] evidenced that the grafting of the triamine reagent onto PA6 led to randomly branched structures. Both reactions of amidification and transamidification can occur with the diamine Jeffamine® D-400. As a result, the same chemical mechanism can be applied for the reagent D-400 and the resulting structures are presented in Figure 2.

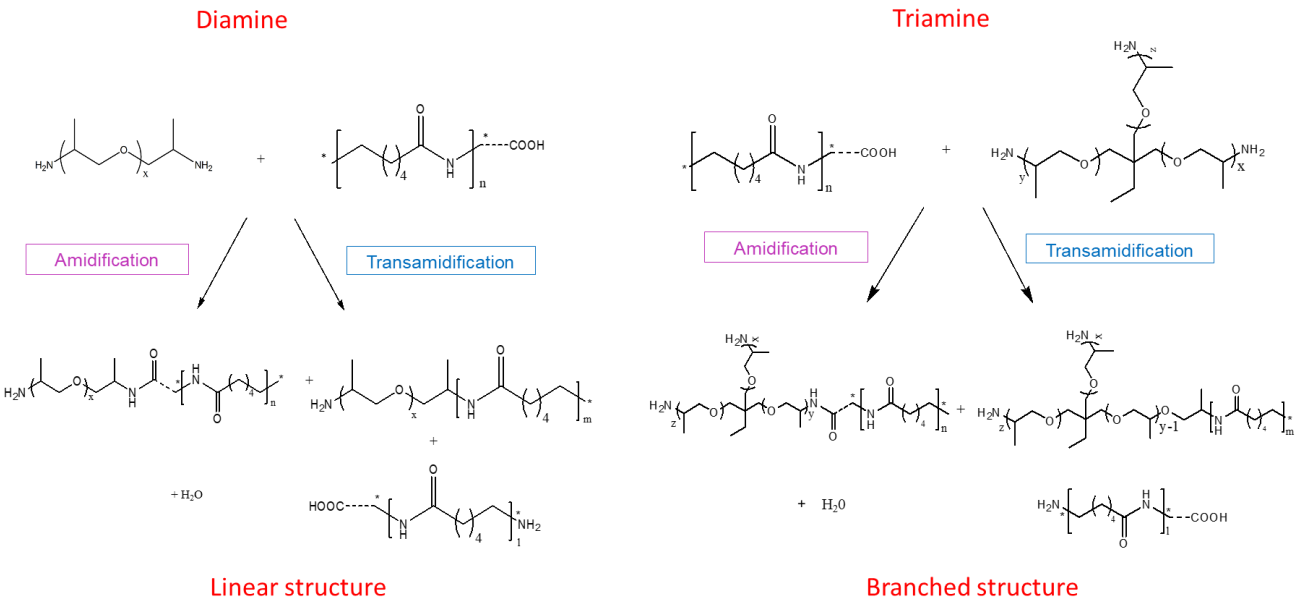

Figure 2: PA6 chain structures from the reaction between PA6 and the diamine or the triamine reagents respectively

Branched structures are obtained with the triamine while linear structures are synthetized using diamine reagents.

IV-a) Physico-chemical properties of the PA6/Jeffamine® reactive blends

Viscosimetry measurements in solution are performed and the results obtained for the two polyetheramine reagents are compared in **Figure 3**.

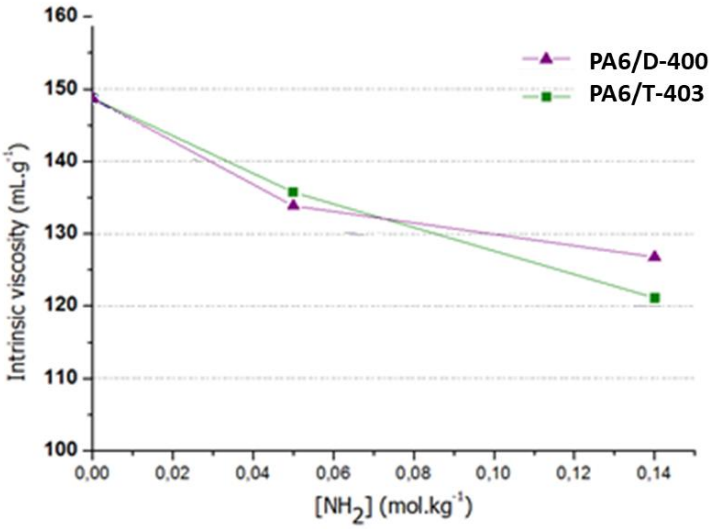

Figure 3: Intrinsic viscosity ([η]) for the different PA6 based reactive systems with different concentrations of injected di- and triamine

For all the reactive blends PA6/T-403 and PA6/D-400, the intrinsic viscosity ([η]) decreases with the addition of amino groups. In the case of D-400, the evolution of [η] (from around 150 $mL.g^{-1}$ to 127 $mL.g^{-1}$) confirms the chemical mechanism proposed previously leading to chain scissions and linear structures [21]. The formation of shorter chains is also confirmed through the SEC analyses results in Table 3, with the continuous decrease of the M_n.

Table 3: Number average molar mass (M_n), weight average molar mass (M_w) and dispersity of the reactive blends measured by SEC in HFIP

Formulations	$[NH_2]_{added}$ ($mol.kg^{-1}$)	M_n ($g.mol^{-1}$)	M_w ($g.mol^{-1}$)	dispersity
Extruded PA6		51,000	11,0000	2.30
PA6/D-400	0.05	36,000	80,000	2.20
	0.14	34,000	78,000	2.30
PA6/T-403	0.05	49,000	100,000	2.00
	0.14	44,000	86,000	2.10

However, for the highest amine concentration (0.14 $mol.kg^{-1}$ of amine added), the intrinsic viscosity of the formulation PA6/D-400 is slightly higher than the one of the formulation PA6/T-403 . This may be due to a difference of hydrodynamic volume of molecules between branched and linear structures. The hydrodynamic volume is lower for branched structure for similar molar mass. The variation of the absolute complex viscosity versus frequency in the molten state of the different formulations are also compared for the different amine concentrations added (Figure 4).

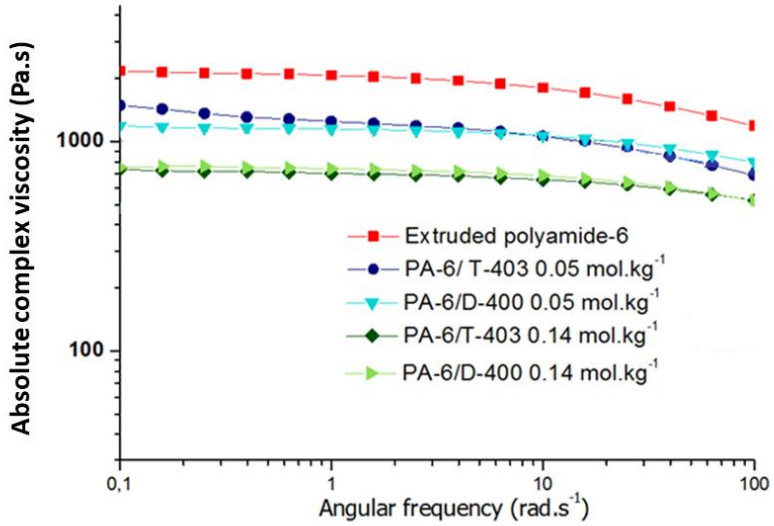

Figure 4: Variation of the absolute complex viscosity of the PA6 and the different reactive blends (T = 240 °C and strain γ = 1 %)

Overall, the complex viscosity of the blends decreases gradually with the Jeffamine® content. For 0.05 mol.kg^{-1} of amine, the viscosity is lowered from 2,000 Pa.s for the virgin PA6 to 1,000 Pa.s for the blends, in accordance with the results found in solution. For 0.14 mol.kg^{-1} of added amine, the complex viscosity decreases also similarly for T-403 and D-400. Besides, the effect of a branched structure compared to their linear counterpart with comparable molar mass was discussed by Risch et al. [26] in their study about the melt viscosity and the crystallization behavior of star-branched PA6. If the number of entanglements per arm is kept low, that is to say, if the chain length is close to the average molar mass between entanglements (5000 g.mol^{-1} for PA6), structures with chain branching exhibited a melt viscosity lower than the equivalent linear one. At 220 °C and for an equivalent weight average molar mass at 31.000 g.mol^{-1}, the zero shear viscosity varies from 600 Pa.s for a linear PA6 to 200 Pa.s for a six-arm PA6 (weight average molar mass of each arm was 7,000 g.mol^{-1} [26, 27]). These phenomena can thus explain the different viscosity behaviors observed.

IV-b) Crystallinity and structural organization in the PA6/T-403 and PA6/D-400 reactive blends

WAXS analyses were first performed to identify the crystalline phases in the both reactive blends (Figure 5). On the pattern, two major crystalline phases are identified (α_1 and α_2) in the formulations and the extruded PA6, meaning that, the reaction between the polyfunctional reagents and PA6 do not modify the crystalline phase nature. To avoid cluttering the graph, the WAXS patterns obtained with 0.14 mol.kg^{-1} of amino groups is not represented but the same conclusion could be drawn.

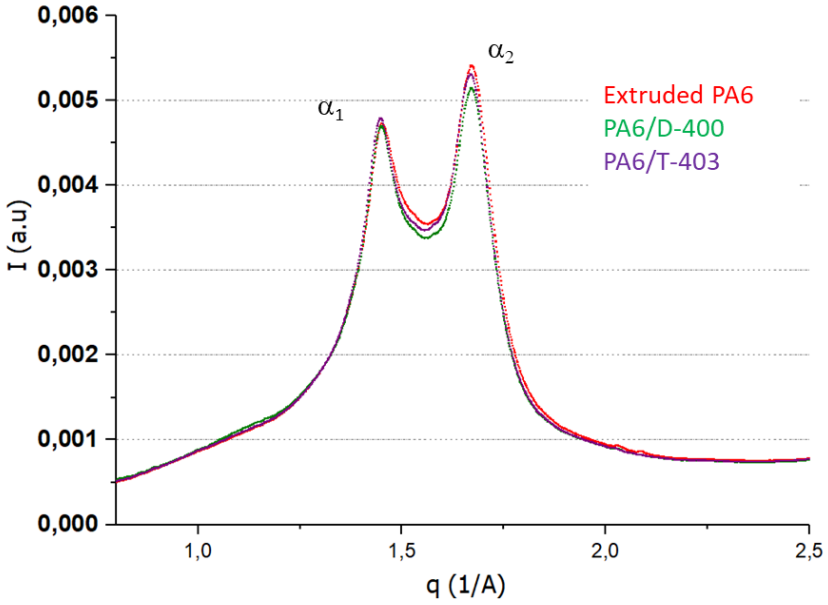

Figure 5: WAXS patterns of the formulations with $[NH_2]$ = 0.05 mol.kg^{-1} of D-400 and T-403

As described in our previous study [21], the crystalline and amorphous lamellae thicknesses are calculated with the long period L_p measured on the SAXS patterns. The χ_c, T_g, RAF and MAF contents are deducted from the modulated DSC analyses. The results are shown in Table 4.

Table 4 Values of the l_c, l_a measured by SAXS and χ_c, T_g and MAF/RAF contents obtained by modulated DSC for the reactive blends PA6/T-403 and PA6/D-400

Formulations	$[NH_2]_{added}$ (mol.kg^{-1})	χ_c (%)	T_g (°C)	L_p (Å)	l_c (Å)	l_a (Å)	MAF (%)	RAF (%)
Extruded PA6	0	32.5 ± 0.2	52.0 ± 0.5	100.5	32.6	67.8	49.4	18.1
PA6/D-400	0.05	**34.9 ± 0.8**	51.9 ± 0.5	100.5	35.1	65.4	47.1	18.0
	0.14	**38.9 ± 0.4**	49.4 ± 0.5	92.7	35.7	60.0	42.8	18.3
PA6/T-403	0.05	**35.2 ± 0.7**	**59.3 ± 0.4**	**102.5**	**36.1**	66.4	40.6	**24.2**
	0.14	**35.0 ± 0.3**	52.1 ± 0.5	95.9	32.7	60.9	42.7	22.3

The first evolution is the higher degree of crystallinity measured for all the blends attributed to the better mobility of shorter chain after transamidification (chain scissions). This phenomenon is even more pronounced for the system based on the reaction of the PA6 with the Jeffamine® D-400. For 0.14 mol.kg^{-1}of NH_2 added, a degree of crystallinity of almost 39 % is observed.

Besides, in our previous study [21], the chain mobility evolution in the amorphous phase was related to the MAF/RAF ratio and the l_a. As mentioned above, for the D-400, the RAF and thickness are almost unchanged compared to the virgin polyamide in our conditions. Compared to the tendency obtained with the reagent T-403 with 0.05 mol.kg^{-1} of NH_2, the RAF is almost unchanged and the l_c increases slightly from 32.6 to around 35 Å. Similarly, the amorphous lamellae thickness barely varies. With [NH_2] = 0.14 mol.kg^{-1}, the only modified parameters are l_a and l_{MAF}. For example, l_a and l_{MAF} decrease from 67.8 to 60.0 Å and 49.6 to 43.2 Å, respectively, for the highest concentration of Jeffamine® D-400. Moreover, the MAF decrease is not significant (maximum 2 %). According to these results and following our reasoning, the T_g of the blend PA6/D-400 at 0.05 mol.kg^{-1} is almost the same as the one of PA6. For the highest D-400 concentration, the shift of T_g may be induced by unreacted small molecules and/or lower molar mass chains as widely described in the literature [28-32]. For 0.14 mol.kg^{-1} of the amine D-400, the plasticization is even more important. At this concentration of amine (0.14 mol.kg^{-1}), the T_g for the D-400 is the lowest because the number of chain scissions is higher, as demonstrated by the viscosimetric and SEC analyses.

In the case of Jeffamine® T-403, the crystalline structure modifications have a predominant effect on the T_g compared to the plasticization induced by the small unreacted molecules and the shorter chains. For the same concentration, the higher content of RAF (respectively lower content of MAF) in the material is observed. The thickening of the RAF phase is explained by the accumulation of branching point at the interface with the crystalline lamella. Lower amorphous phase mobility is noticed for the material modified with the lowest amount of amine functions (0.05 mol.kg^{-1}) as its glass transition temperature increases by approximately 7 °C. The higher RAF hinders the mobility of chains in the amorphous phase by a confinement effect. This point was confirmed by Parodi et al. [23] studying the impact of the crystalline structure modified after thermal treatment on the glass transition temperature. The thermal history affects the MAF/RAF ratio directly linked to the chain mobility in the amorphous phase. For a continuous crystallization, if the MAF decreases from 60 to 40 %, the T_g increases from 71 to 76 °C. Overall and contrary to what was seen with the reagent T-403, the reaction between the diamine reagents and PA6 did not modify significantly the nano-structure of the material and especially the RAF proportion. The impact of the nano-structure evolution (particularly the RAF) is represented in Figure 6.

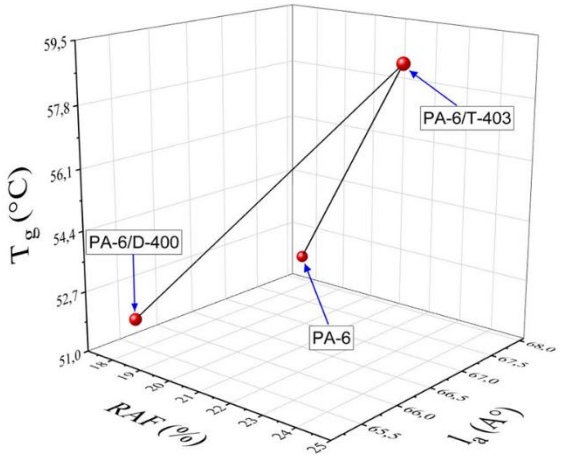

Figure 6: 3D graph representation of the link between T_g, %RAF and l_a for $[NH_2] = 0.05$ mol.kg^{-1}

It is of importance to emphasize the fact that this relationship between the T_g and the crystalline organization is observed in the literature for polymer structures modified by thermal treatment e.g. annealing and not by chemical reaction. Thus, the link between the layers thickness/RAF and T_g is a plausible theory if formulations have a low amount of reagent, that is to say, if the polymer is slightly chemically modified and almost not plasticized.

To sum up, two main parameters affect the T_g of the materials: the MAF/RAF by confinement effect and the amorphous phase composition if chemical reactions occurred and/or a sufficient amount of unreacted molecules is added to the polymer and localized in the amorphous phase.

IV-c) Tensile properties of the PA6/T-403 and PA6/D-400 reactive blends

The tensile properties and the glass transition temperatures for all different reactive blends are presented in Table 5.

Table 5: Tensile properties and glass transition temperatures of reactive blends PA6/T-403 and D-400

Formulations	Amine added (wt%)	$[NH_2]_{added}$ ($mol.kg^{-1}$)	χ_c (%)	T_g (°C)	Young's modulus (MPa)	Yield strength (MPa)	Elongation at break (%)
Extruded PA6	0	0	32.5 ± 0.2	52.0	1,000 ± 10	77 ± 1	380 ± 3.0
PA6/D-400	1.0	0.05	**34.9 ± 0.8**	51.9	1,080 ± 14	81 ± 0	130 ± 70
	2.9	0.14	**38.9 ± 0.4**	49.4	1030 ± 10	72 ± 0	140 ± 40
PA6/T-403	0.70	0.05	**35.2 ± 0.7**	**59.3**	**1,200 ± 10**	**87 ± 1**	360 ± 35
	2.0	0.14	**35.0 ± 0.3**	52.1	**1,100 ± 8**	76 ± 3	380 ± 30

The reactive blends elaborated with diamines, and for the lowest amine concentrations, exhibites a slight increase of the Young's modulus and yield strength compared to those measured for the neat PA6. For this formulations, the slight increase of the material stiffness compared to PA6 alone could be induced by higher crystallinity and thicker crystalline layers (respectively thinner amorphous lamellae). However, this enhancement is limited compared to the values reached with the triamine. As an example, for $[NH_2]$ = 0.05 $mol.kg^{-1}$, the Young's modulus was measured at 1,200 MPa for the triamine and 1080 MPa for the D-400. The major difference concerns the elongation at break which dropped dramatically with the addition of small concentrations of diamine. At 0.14 $mol.kg^{-1}$ of D-400, the elongation at break decreases to 140 % which is explained by the higher crystalline ratio attributed to lower molar masses.

The material stiffening, in spite of a constant or lower molar mass, is often attributed to higher degrees of crystallinity [29, 30]. As an example, Starkweather et al. [31] demonstrated that, independently of the tested molar mass, the stiffness of a PA6 increased from 550 to 830 MPa for higher degree of crystallinity from 10 to 25 % (induced by thermal treatment). However, and as discussed previously, the degree of crystallinity is not the only factor affecting the tensile properties; otherwise the materials made with the diamines would be stiffer than those with the triamine, particularly at 0.14 $mol.kg^{-1}$ of amine.

In order to explain the improved tensile properties obtained with the addition of small amount of T-403, the crystalline parameters studied previously have to be considered [21, 33, 34]. Numerous studies explained the mechanical behavior of semi-crystalline polymers with

the crystalline nature and the lamellae thicknesses [33, 35-38]. To illustrate this point, Kolesov et al. [25] highlighted the tensile properties difference observed between the α- and γ-phase obtained by different crystallization conditions on PA6. The elastic modulus of the α-phase was estimated at around 300 GPa while the one of the γ-phase was between 50 and 140 GPa.

Some research teams attributed the improvement of the tensile properties to an increase of the thickness of the crystalline lamellae in the case of polyolefin [34, 35, 39]. For example, Menyhárd et al. [40] simulated successfully the relationship between the tensile properties and l_c for five isotactic polypropylenes. For a fixed degree of crystallinity (χ_C = 50 %), the modulus increased by 0.4 GPa for thicker l_c from 20 to 40 nm. Only few studies pointed out the crucial role of l_a on the mechanical response of polymers. Kennedy et al. [38] pointed out that, in the pre-yield region, the deformation involves first the non-crystalline parts of the material before damaging the crystalline layers. As a consequence, the thickness of the amorphous lamellae should be considered. For linear polyethylene, the initial modulus was directly linked to the interlamellar thickness evolution with two distinctive regions defining the brittle to ductile transition.

Most papers investigated the mechanical properties above the T_g and demonstrated that, l_a has a particular importance. In our case, the samples were analyzed below the T_g so, in this case, the contribution of the crystalline and amorphous phase separately are not so distinguishable.

As a result, it is indeed exceptional to observe both an increase in modulus and yield stress, while also having an increase in elongation at break. For a homogeneous medium, the explanation may lie in the presence of unreacted molecules. Nevertheless, we did not specifically evaluate the unreacted molecules and this hypothesis, based on a plasticization phenomenon, is not entirely convincing due to the very low concentration of unreacted molecules. It can only be argued that these star-shaped structures of the PA6 chains lead to a nanostructured material of a different nature compared to the virgin PA6.

With the system PA6/T-403 containing the lowest concentration of amino groups (0.05 $mol.kg^{-1}$), both modifications are particularly important: thickening of the crystalline lamellae (from 32.6 to 36.1 Å) and the higher RAF (from 18.1 to 24.2 %). The higher l_c in the sample PA6/T-403 could partly explain the better tensile properties compared those of the neat polyamide. Moreover, the higher rigidity of the amorphous phase brought by the increase of the RAF should impact the global stiffness of the material. Finally, the higher degree of crystallinity (from 32.5 to 35.2 %) may also contribute to the stiffening of the material.

For the formulation with 0.14 $mol.kg^{-1}$ of Jeffamine® T-403, l_c is almost not modified but l_a decreases and the RAF increases by 5-6 % compared to the structural parameters of the neat polyamide. The tensile properties should have been higher but the material starts being plasticized at this concentration [21].

The reactive blends PA6/T-403 exhibited particular and interesting properties for a very small amount of reagent. Indeed, the formulation with 0.05 mol.kg^{-1} of amino groups combines the benefits of a lower viscosity, better tensile properties and a higher T_g compared to the virgin PA6. These particular properties are attributed to the ability of branched chains to greatly contribute to the material nano-structure and impact the amorphous phase mobility. The higher rigidity of the amorphous phase brought by higher RAF impacts the global stiffness of the material. This relationship is finally represented through a 3D graph in Figure 7.

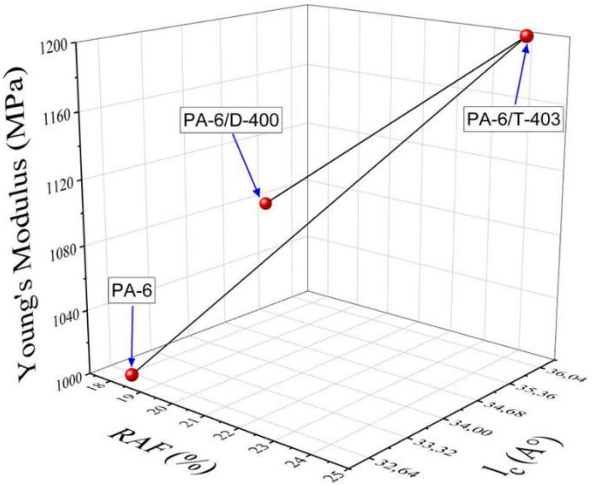

Figure 7: 3D graph representation of the link between the Young's modulus, %RAF and l_c ([NH_2] = 0.05 mol.kg^{-1} with the same χ_c and l_a) for the reactive blends

For the blend with 0.14 mol.kg^{-1} of amine D-400, both χ_C and l_c kept increasing while l_a decreases and the ratio RAF/MAF is unchanged. Logically, the Young's modulus and the yield strength should be better than the one of the blend PA6/D-400 with 0.05 mol.kg^{-1} of amine. This is not the case because, as observed with the T-403, the unreacted molecules promote the amorphous phase mobility decreasing their tensile properties.

These results prove that, under our experimental conditions, the crystalline/amorphous phase thicknesses and the RAF/MAF contents have to be considered to explain the tensile properties. Modulated DSC measurements prove that the branching points created by the reaction of a low percentage of trifunctional additives onto PA6 induce a specific crystalline microstructure responsible for the better tensile properties observed.

The properties evolutions (tensile behaviour and T_g) are linked to nano-structure evolutions induced by the chemical reactions occurring between the reagents and PA6. It has been demonstrated that the branching points, introduced by the triamine, induce significant modifications of the crystallinity (dimension and composition). On the contrary, the reaction with diamine leads to linear chains and do not modify noticeably the crystalline structure at

the nanometric scale. A schematic representation of the crystalline structure evolution is proposed in the case of the triamine or diamine reagents (Figure 8).

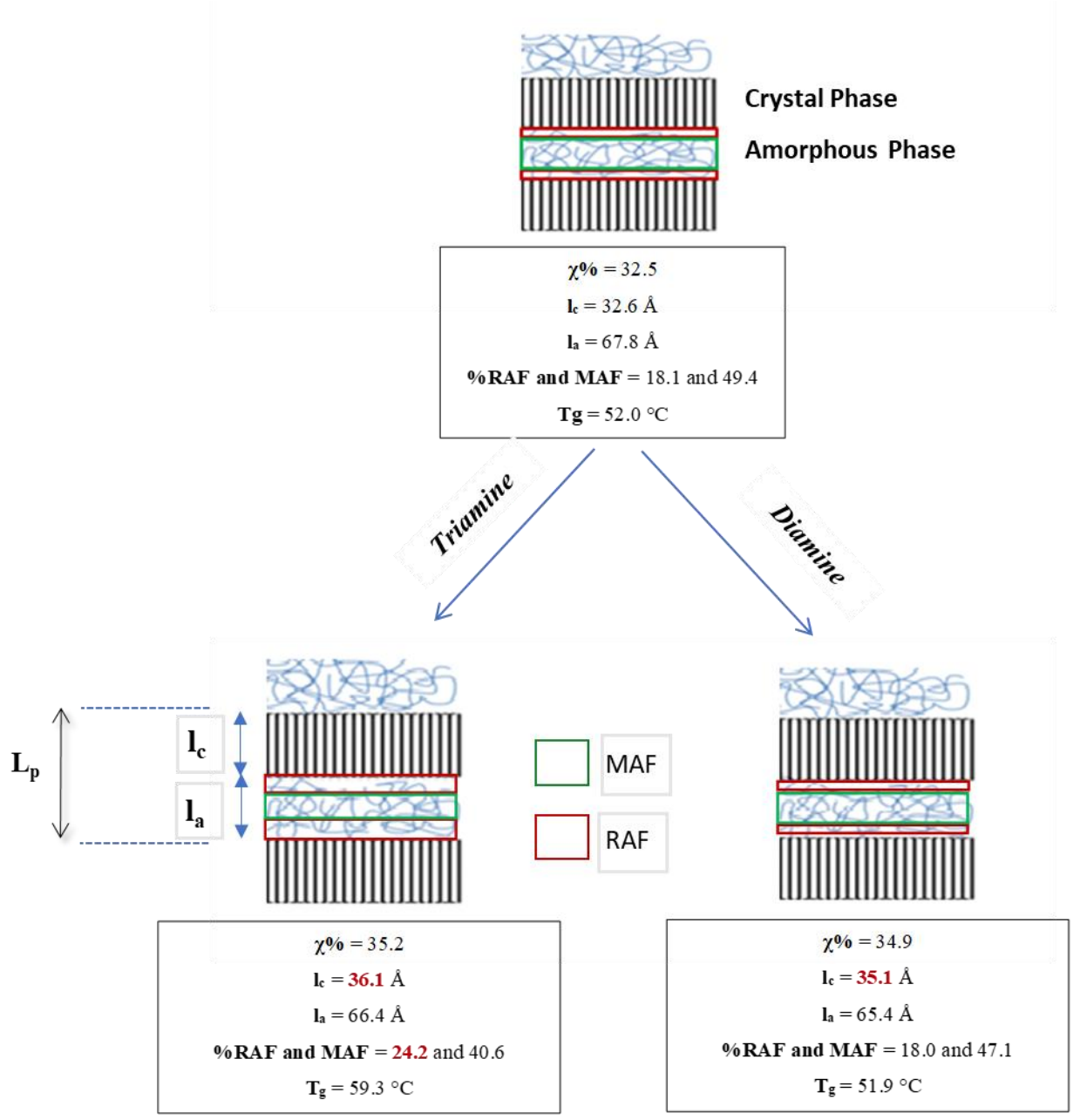

Figure 8: Comparison of the nano-structures obtained after reaction with the triamine or diamine for $[NH_2]$ = 0.05 mol.kg^{-1}

The branching points obtained by adding the triamine T-403 may be accumulated at the interface with the crystalline lamellae. As a result, an important increase of the RAF (content and thickness) is observed in this case compared to the unmodified PA6. The higher amount of this rigid phase might hinder some chain motions increasing the T_g. For the reactive blends with diamines, no modification is noticed regarding the RAF/MAF contents.

The diamine molecules present in the amorphous phase plasticize the material, hence the T_g decreases. Regarding the tensile properties, the slight improvement observed for the blends PA6/D-400 is attributed to both higher crystalline fraction and thicker crystalline lamellae (~ + 2.5 Å). In addition to these modifications and as explained previously, the reactive blends PA6/T-403 has a higher RAF which influence the global stiffness of the material and explain the better mechanical performances observed compared to the others formulations.

Conclusions

This study presents two different systems using triamine or diamine type reagents (triamine Jeffamine® T-403 and a diamine Jeffamine®D-400) to modify PA6 by reactive extrusion. The material containing branching points introduced by the three-branched polyether amine provides interesting properties as it combined lower viscosity and higher mechanical/thermo-mechanical performances compared to the neat PA6. These characteristics are reached thanks to the particular ability of these branched molecules to nano-structure the polyamide. Actually, the formation of randomly branched structures resulted in important modifications of the nano-structure (l_c of 36.1 Å and a RAF of 24,2%), while the linear structures created by addition of diamines did not induce any noticeable variation at this scale. Comparing the results obtained by DSC, SAXS and tensile tests, we established the relationships between the T_g, the tensile properties and the crystalline structure parameters of the materials. Deeply, we demonstrated that the RAF and MAF variations affect the chain mobility in the amorphous phase of the material. Indeed, higher RAF and/or lower MAF induced a loss of chain mobility in the amorphous phase due to the confined effect imposed by the surrounding rigid phase. As an example, for 0.05 $mol.kg^{-1}$ of amine T-403, an increase of the RAF by 6 % led to a higher T_g (~ + 7 °C). In the case of Jeffamine® D-400 no structural modifications were observed. In our specific experimental conditions, the crystalline/amorphous layers thicknesses, the crystallinity and again the RAF/MAF ratio were the most influential parameters on the tensile properties. Larger crystalline lamellae but also higher RAF and crystal content can strengthen the material. For the blend PA6/T-403 (0.05 $mol.kg^{-1}$), the Young's modulus and the yield strength was improved by 20 and 13 % respectively due to higher RAF (~ + 6 %) and thicker l_c (~ + 3.5 Å).

ACKNOWLEDGEMENTS

The authors thank Adrien Tauleigne for his help during the extrusion process, Marion Colella for her technical assistance regarding the SEC analyses, Isabelle Morfin for her assistance with the SAXS and WAXS experiments [the Wide-angle X-ray detector (WOS) was funded by the French National Research Agency (ANR) under the ''Investissement d'Avenir'' program (Grant no. ANR-11-EQPX-0010)]. The authors are grateful to the laboratory IMP/HUTCHINSON for the financial support.

REFERENCES

[1] Pervaiz, M.; Faruq, M.; Jawaid, M.; Saina, M. Polyamides: Developments and Applications Towards Next Generation Engineered Plastic, Curr. Org. Synth., 14, (2017), 146-155. doi: 10.2174/1570179413666160818144816

[2] Marchildon, K. Polyamides – Still Strong After Seventy Year, Macromol. React. Eng. 5 (2011), 22–54. doi: 10.1002/mren.20100001

[3] Wesolowski, J.; Plachta, K. Market for Polyamides, Fibres and Textiles in Eastern Europe, 24, 6, (2017) 12-18 doi:10.5604/12303666.1221737

[4] Lee, J.; Seo, W.G.; Kim, J.; Kim, Y.S.; Yoo, Y.; Moon, J.H.; Kim, S.G.; Jung, H.M. Amide-based oligomers for low-viscosity composites of polyamide 66, Macromol. Res., 25 Issue 10 (2017) 1598-5032 doi:10.1007/s13233-017-5129-2

[5] Warakomski, J.M. Synthesis and properties of star-branched nylon 6, Am. Chem. Soc. Polym. Prepr. Div. Polym. Chem. 30 (1989) 117–118. doi:10.1021/cm00023a014.

[6] Hashimoto, K. Ring-opening polymerization of lactams. Living anionic polymerization and its applications, Prog. Polym. Sci. 25 (2000) 1411–1462. doi:10.1016/S0079-6700(00)00018-6.

[7] Piskun, Y.A.; Vasilenko, I.V.; Gaponik, L.V.; Kostjuk, S.V. Activated anionic ring-opening polymerization of ε-caprolactam with magnesium di(ε-caprolactamate) as initiator: Effect of magnesium halides, Polym. Bull. 68 (2012) 1501–1513. doi:10.1007/s00289-011-0621-x.

[8] Fu, P.; Wang, M.; Liu, M.; Jing, Q.; Cai, Y.; Wang, Y.; Zhao, Q. Preparation and characterization of star-shaped nylon 6 with high flowability, J. Polym. Res. 18 (2011) 651–657. doi:10.1007/s10965-010-9460-y.

[9] Puskas, J.E.; Paulo, C.; Altstadt V. Mechanical and viscoelastic characterization of hyperbranched polyisobutylenes, Rubber Chem. Technol. 75 (2002) 853–863. doi:10.5254/1.3547688.

[10] Run, M.; Wang, J.; Yao, M.; Guo, L.; Wang, H.J.; Ba, X. Influences of hyperbranched poly(amide-ester) on the properties of poly(butylene succinate), Mater. Chem. Phys. 139 (2013) 988–997. doi:10.1016/j.matchemphys.2013.02.068.

[11] Massa, D.J.; Shriner, K.A.; Turner, S.R.; Voit, B.I. Novel blends of hyperbranched polyesters and linear polymers, Macromolecules. 28 (1995) 3214–3220. doi:10.1021/ma00113a025.

[12] Fan, Z.; Jaehnichen, K.; Desbois, P.; Haeussler, L.; Vogel, R.; Voit, B. Blends of different linear polyamides with hyperbranched aromatic AB_2 and A_2+B_3 polyesters, J. Polym. Sci. 47 (2009) 558-3572. doi:10.1002/pola.23440.

[13] Tang, X.; Kong, Q. Synthesis and characterization of the hyperbranched polyamide with triphenyl phosphorus structure and the influence on mechanical property of nylon-6, Adv. Mater. Res. 830 (2015) 2–7. doi:10.4028/www.scientific.net/AMR.830.167.

[14] Huber, T.; Pötschke, P.; Pompe, G.; Häßler, R.; Voit, B.; Grutke, S.; Gruber, F. Blends of hyperbranched poly(ether amide)s and polyamide-6, Macromol. Mater. Eng. 280–281 (2000) 33–40. doi:10.1002/1439-2054(20000801)280:1<33::AID-MAME33>3.0.CO;2-P.

[15] Monticelli, O.; Oliva, D.; Russo, S.; Clausnitzer, C.; Pötschke, P.; Voit, B. On blends of polyamide 6 and a hyperbranched aramid, Macromol. Mater. Eng. 288 (2003) 318–325. doi:10.1002/mame.200390033.

[16] Kersch, M.; Schmidt, H.W.; Altstädt, V. Influence of different beta-nucleating agents on the morphology of isotactic polypropylene and their toughening effectiveness, Polym. (United Kingdom). 98 (2016) 320–326. doi:10.1016/j.polymer.2016.06.051.

[17] Steeman, P.; Nijenhuis, A. The effect of random branching on the balance between flow and mechanical properties of polyamide-6, Polymer (Guildf). 51 (2010) 2700–2707. doi:10.1016/j.polymer.2010.04.017.

[18] Cai, J.; Liu, Z.; Cao, B.; Guan, X.; Liu, S.; Zhao, J. Simultaneous improvement of the processability and mechanical properties of the polyamide-6 by chain extension in extrusion, Ind. Eng. Chem. Res. , 59 (2020),14334-14343 doi:10.1021/acs.iecr.0c02022

[19] Seo, Y.P.; Seo, Y. Effect of molecular structure change on the melt rheological properties of a polyamide (nylon 6), ACS Omega, 3 (2018), 16549-16555 doi:10.1021/acsomega.8b02355

[20] Lucas, A.; Tauleigne, A.; Da Cruz-Boisson, F.; Crepet, A.; Bergeron-Vanhille, A.; Martin, G.; Garois, N.; Cassagnau, P.; Bounor-Legaré, V. Mechanical Properties Enhancement while Decreasing the Viscosity of Copolyether-Ester from In Situ Formation of Star-Based Structures by Reactive Extrusion, Ind. Eng. Chem. Res., 59 (2020),16579-16590 doi:10.1021/acs.iecr.0c02801

[21] Auclerc, M.; Tauleigne, A.; Da Cruz Boisson, F.; Vanhille Bergeron, A.; Garois, N.; Fulchiron, R.; Sudre, G.; Cassagnau, P.; Bounor-Legaré, Polyamide-6 structuration induced by a chemical reaction with a polyether triamine in the molten state, Polymer, 172 (2019), 339-354 doi:10.1016/j.polymer.2019.03.033

[22] Kiziltas, E.E.; Yang, H.S.; Kiziltas, A.; Boran, S.; Ozen, E.; Gardner, D.J. Thermal analysis of polyamide 6 composites filled by natural fiber blend, BioResources, 11 (2016) 4758–4769. doi:10.15376/biores.11.2.4758-4769.

[23] Parodi, E.; Govaert, L.E.; Peters, G.W.M. Glass transition temperature versus structure of polyamide 6: A flash-DSC study, Thermochim. Acta. 657 (2017) 110–122. doi:10.1016/j.tca.2017.09.021.

[24] ATHAS data bank, http://web.utk.edu/athas/databank/amide/nylon6/, Ed., M. Pyda, 1997

[25] Huang, Y.; Paul, D.R. Effect of molecular weight and temperature on physical aging of thin glassy Poly(2,6-dimethyl-1,4-phenylene oxide) Films, J. Polym. Sci. Part B Polym. Phys. 45 (2007) 1390–1398. doi:10.1002/polb.

[26] Risch, B.G.; Wilkes, G.L.; Warakomski, J.M. Crystallization kinetics and morphological features of star-branched nylon-6: effect of branch-point functionality, Polymer (Guildf). 34 (1993) 2330–2343. doi:10.1016/0032-3861(93)90817-T.

[27] Flory, J. Synthesis of Multichain Polymers and Investigation of their Viscosities, J. Am. Chem. Soc. 241 (1948) 2709–2718. doi:10.1021/ja01188a026.

[28] Suvorova, A.I.; Khannanova, E.G. Molecular structure of plasticizers and antiplasticization, Macromol. Chem. Phys. 191 (1990) 993–998. doi:10.1002/macp.1990.021910501.

[29] Moffatt, S.; Ajji, A.; Lotz, B.; Brisson, J. Uniaxial deformation of nylon-6 and nylon-11: Changes in orientation and crystal phase, Can. J. Chem. 76 (1998) 1491–1500. doi:10.1139/v98-121.

[30] Mazan, T.; Berggren, R.; Jorgensen, J.K.; Echtermeyer, A. Aging of polyamide 11. Part 1: Evaluating degradation by thermal, mechanical, and viscometric analysis, J. Appl. Polym. Sci. 132 (2015). doi:10.1002/app.41971.

[31] Starkweather, H.W.; Moore, G.E.; Hansen, J.E.; Roder, T.M.; Brooks R.E. Effect of crystallinity on the properties of nylons, J. Polym. Sci. 21 (1956) 189–204. doi:10.1002/pol.1956.120219803.

[32] Guo, C.; Zhou, L.; Lv, J. Effects of expandable graphite and modified ammonium polyphosphate on the flame-retardant and mechanical properties of wood flour-polypropylene composites, Polym. Polym. Compos. 21 (2013) 449–456. doi:10.1177/096739111302100706

[33] Fatahi, S.; Ajji, A.; Lafleur, P.G. Correlation Between Different Microstructural Parameters and Tensile Modulus of Various Polyethylene Blown Films, Polym. Eng. Sci. 47 (2007) 1430–1440. doi:10.1002/pen.20836.

[34] Kolesov, I.; Mileva, D.; Androsch, R. Mechanical behavior and optical transparency of polyamide 6 of different morphology formed by variation of the pathway of crystallization, Polym. Bull. 71 (2014) 581–593. doi:10.1007/s00289-013-1079-9.

[35] Crist, B.; Fisher, C.J.; Howard, P.R. Mechanical properties of model polyethylenes: tensile elastic modulus and yield stress, Macromolecules, 22 (1989) 1709–1718. doi:10.1021/ma00194a035.

[36] Millot, C.; Séguéla, R.; Lame, O.; Fillot, L.A.; Rochas, C.; Sotta, P. Tensile deformation of bulk Polyamide 6 in the preyield strain range. Micro-macro strain relationships via in situ SAXS and WAXS, Macromolecules, 50 (2017) 1541–1553. doi:10.1021/acs.macromol.6b02471.

[37] Nitta, K.; Yamaguchi, N. Influence of morphological factors on tensile properties in the pre-yield region of Isotactic polypropylenes, Polym. J. 38 (2006) 122–131. doi:10.1295/polymj.38.122.

[38] Kennedy, M.A.; Peacock, A.J.; Mandelkern, L. Tensile properties of crystalline polymers: linear polyethylene, Macromolecules, 27 (1994) 5297–5310. doi:10.1021/ma00097a009.

[39] Doyle, M.J. On the effect of crystallinity on the elastic properties of semicrystalline polyethylene, Polym. Eng. 4 (2000) 0–5. doi:10.1002/pen.11166.

[40] Menyhárd, A.; Suba, P.; László, Z.; Fekete, H.M.; Mester, O.; Horváth, Z.; Vörös, G.; Varga, J.; Móczó, J. Direct correlation between modulus and the crystalline structure in isotactic polypropylene, Express Polym. Lett. 9 (2015) 308–320. doi:10.3144/expresspolymlett.2015.28.